Release Profiles of Encapsulated Actives from Colloidosomes Sintered for Various Durations

Huai Nyin Yow and Alexander F. Routh*

Department of Chemical Engineering and Biotechnology, BP Institute, University of Cambridge, Madingley Road, Cambridge CB3 0EZ, United Kingdom

Received August 19, 2008. Revised Manuscript Received October 17, 2008

This paper presents the formation of low temperature colloidosomes from colloidal poly(styrene-*co*-butyl acrylate) particles for both water-in-oil and oil-in-water systems. An investigation into the sintering conditions examines the ultimate shell morphology formed, with longer sintering times and higher sintering temperatures producing less porous microcapsules. This has been verified by the release of an encapsulated dye from the aqueous core microcapsules, in which slower release has been detected for longer sintering times. The results are subsequently fitted with a diffusion equation to give a diffusion coefficient of fluorescein through the polymeric shell of 10^{-17} m^2/s.

1. Introduction

Microencapsulation is a process in which gases, liquid droplets, or solid particles (the core) are isolated by embedding or surrounding the core in another substance (the matrix or shell). Microencapsulation has been used in various products, including food and beverages,[1] biotechnology,[2] textiles,[3] and many others. This has been accomplished using a diverse number of techniques and materials, with varying release mechanisms.[4] In this paper, emphasis is given on using a polymeric substance as the surrounding shell.

Recently, the technique of self-assembly of colloidal particles at the water/oil interface was introduced by Velev et al.,[5−7] while Dinsmore et al.[8,9] coined the phrase "colloidosomes", describing microcapsules with shells of coagulated/fused colloidal particles. This was further developed into "hairy" colloidosomes,[10] "carbon nanotubosomes",[11] composite colloidosomes,[12−14] and responsive colloidosomes.[15,16] Its wide applicability sparked interest in understanding colloidosomes as an encapsulation vessel. The inherent interstices between the colloidal particles in the shell govern the release of the encapsulated actives, and hence the success of colloidosomes in encapsulation.

This paper expands on the work by Laïb and Routh,[17] looking into the formation of water-in-oil and oil-in-water colloidosomes at different sintering conditions. It also reports on the encapsulation of a hydrophilic dye within the water-in-oil microcapsules and tracks the release of this active by spectrophotometry. A diffusion equation is fitted to the experiments to estimate the diffusion coefficient of dye through the polymeric shell. Generally, the release profile for an encapsulated ingredient is controlled by the molecular size and solubility of the active within the shell, the properties of microcapsules (including size, shell thickness, and shell permeability), and the nature of the release medium.[18]

2. Experimental

2.1. Materials. Butyl acrylate (Aldrich, 99+%) was purified by vacuum distillation prior to use, while styrene (Acros Organics, 99%) was purified by filtration through aluminum oxide (Fisher Scientific, general purpose grade) and two layers of filter paper. The following were used without purification: acrylic acid (Acros Organics, 99.5%), potassium persulphate (BDH, 98%), sodium dodecyl sulfate (SDS) (Aldrich, 98%), sunflower oil (Tesco), Span 80 (Fluka), Tween 20 (Acros Organics), and fluorescein sodium salt (Fluka).

2.2. Methods. *2.2.1. Synthesis of Poly(styrene-co-butyl acrylate) Particles.* The latex particles were synthesized by emulsion polymerization.[19] A 3 L three neck round-bottom flask was equipped with a glass link stirrer, reflux condenser, and nitrogen gas inlet. The flask was immersed in a water bath at 85 °C and purged with nitrogen gas for 20 min. While under nitrogen, distilled water (600.0 mL) and half of the monomers [styrene (160.0 g), butyl acrylate (87.5 g), and acrylic acid (2.5 g)] were added into the flask and stirred at 300 rpm for 5 min. Potassium persulphate (0.03 g in 10.0 mL distilled water) and SDS (1.0 g in 10.0 mL of distilled water) were subsequently added to initiate polymerization. The reaction was allowed to progress for 20 min, and then the remaining distilled water (580.0 mL) and monomers [styrene (160.0 g), butyl acrylate (87.5 g), and acrylic acid (2.5 g)] were added. The nitrogen was turned off after another 20 min, and the system was isolated with the reaction allowed to continue overnight. The product was a milky white suspension, which was dialyzed for a week with daily water

* E-mail: afr10@cam.ac.uk.

(1) Gibbs, B. F.; Kermasha, S.; Alli, I.; Mulligan, C. N. *Int. J. Food Sci. Nutr.* **1999**, *50*, 213–224.
(2) Chang, T. M. S.; Prakash, S. *Mol. Biotechnol.* **2001**, *17*, 249–376.
(3) Zydowicz, N.; Nzimba-Ganyanad, E.; Zydowicz, N. *Polym. Bull.* **2002**, *47*(5), 457–463.
(4) Yow, H. N.; Routh, A. F. *Soft Matter* **2006**, *2*, 940–949.
(5) Velev, O. D.; Furusawa, K.; Nagayama, K. *Langmuir* **1996**, *12*, 2374–2384.
(6) Velev, O. D.; Furusawa, K.; Nagayama, K. *Langmuir* **1996**, *12*, 2385–2391.
(7) Velev, O. D.; Furusawa, K.; Nagayama, K. *Langmuir* **1997**, *13*, 1856–1859.
(8) Dinsmore, A. D.; Hsu, M. F.; Nikolaides, M. G.; Marquez, M.; Bausch, A. R.; Weitz, D. A. *Science* **2002**, *298*, 1006–1009.
(9) Hsu, M. F.; Nikolaides, M. G.; Dinsmore, A. D.; Bausch, A. R.; Gordon, V. D.; Chen, X.; Hutchinson, J. W.; Weitz, D. A.; Marquez, M. *Langmuir* **2005**, *21*, 2963–2970.
(10) Noble, P. F.; Cayre, O. J.; Alargova, R. G.; Velev, O. D.; Paunov, V. N. *J. Am. Chem. Soc.* **2004**, *126*, 8092–8093.
(11) Panhuis, M.; Paunov, V. N. *Chem. Commun.* **2005**, *13*, 1726–1728.
(12) He, Y. J.; Li, T. H.; Yu, X. Y.; Zhao, S. Y.; Lu, J. H.; He, J. *Appl. Surf. Sci.* **2007**, *253*, 5320–5324.
(13) Bon, S. A. F.; Colver, P. J. *Langmuir* **2007**, *23*, 8316–8322.
(14) Kim, S. H.; Heo, C. J.; Lee, S. Y.; Yi, G. R.; Yang, S. M. *Chem. Mater.* **2007**, *19*, 4751–4760.
(15) Lawrence, D. B.; Cai, T.; Hu, Z.; Marquez, M.; Dinsmore, A. D. *Langmuir* **2007**, *23*, 395–398.
(16) Kim, J.-W.; Fernandex-Nieves, A.; Dan, N.; Utada, A. S.; Marquez, M.; Weitz, D. A. *Nano Lett.* **2007**, *7*, 2876–2880.
(17) Laib, S.; Routh, A. F. *J. Colloid Interface Sci.* **2007**, *317*, 121–129.
(18) Dowding, P. J.; Atkin, R.; Vincent, B.; Bouillot, P. *Langmuir* **2005**, *21*(12), 5278–5284.
(19) Sperry, P. R.; Snyder, B. S.; O'Dowd, M. L.; Lesko, P. M. *Langmuir* **1994**, *10*, 2619–2628.

10.1021/la802711y CCC: $40.75
Published on Web 12/08/2008

changes. The cleaned latex particle suspension was subsequently adjusted to a concentration of 5.6 wt %.

2.2.2. Characterization of Latex Particles. The latex particles were imaged by scanning electron microscopy (SEM). A JEOL-6340F Field Emission Gun SEM was used at an accelerating voltage of 5.0 kV. A drop of particle suspension was air-dried on a stainless steel SEM stub overnight. The sample was then platinum-coated using an Emitech K575 sputter coater, in an argon environment at 1×10^{-3} mbar and 40 mA for 1 min.

The latex particles were also sized by dynamic light scattering (DLS) (Brookhaven ZetaPlus), coupled to particle sizing software (Brookhaven, version 3.42). A drop of particle suspension (approximately 0.1 mL) was placed in a disposable plastic cell and diluted to 3.0 mL of virtually clear solution. The effective diameter obtained was accurate to ±1%, with the reported value being the average of 10 measurements.

To measure the minimum film formation temperature (MFFT), a MFFT bar was used. The colloidal suspension was spread at a thickness of 1 mm on a glass bar of 68 × 16.5 cm. The glass bar had been previously placed on the MFFT bar with temperature varying from 20 to 70 °C across the bar length. Air flow was forced across the surface from the cold to hot end. The setup was left for 2 h; a film was formed, and the MFFT was measured with an on-board thermocouple. The MFFT was defined as the temperature at which the polymer particles deform to form a homogeneous film.[20] This is represented by the condition at which the film appearance changes from a cloudy white cracked film in the cold section of the MFFT bar to a clear transparent film in the hotter section.

2.2.3. Fabrication of Water-in-Oil Colloidosomes. Span 80 (4 mL) was mixed with sunflower oil (200 mL) for 5 min in a 400 mL beaker with a Silverson high shear mixer (model SL2) at 3000 rpm. The latex particle suspension (2 mL) was then added over 30 s. Cyclic mixing was employed, whereby homogenization was carried out for 60 s, followed by 30 s rest. This was repeated five times. After emulsification, the emulsion was separated into five tubes and heated in a water bath at 50 ± 0.5 °C. The temperature was stabilized before sintering was considered to have initiated. This took between 10 and 12 min. Once the temperature had reached 49 ± 0.5 °C, the timer was started and the emulsions were sintered for 5, 15, 30, 45, and 60 min, respectively. In certain experiments, a 40 mL emulsion tube was kept without heating, denoted as nonsintered. The duration and temperature at which heating was maintained are represented as sintering time, t_s, and sintering temperature, T_s. After sintering, the tubes were left for three days at ambient conditions. This allowed the microcapsules to sediment. Five milliliters of the white sediment was then transferred into an empty centrifuge tube and washed with MilliQ water (18.2 MΩ•cm). The mixture was centrifuged at 10 000 rpm for 10 min at 20 °C. The creamed oil was removed via pipetting, and the microcapsules, redispersed in an aqueous phase, were characterized.

2.2.4. Fabrication of Oil-in-Water Colloidosomes. Tween 20 (1.6 mL) was added to the latex particle suspension (80 mL). The mixture was stirred in a 250 mL beaker with a Silverson stirrer for 5 min at 6000 rpm. Sunflower oil (0.8 mL) was then added over 30 s. Cyclic mixing was again employed, whereby emulsification was maintained for 60 s, followed by 30 s rest. This protocol was repeated five times. After emulsification, the emulsion was divided into four tubes. One tube was kept without sintering, denoted as nonsintered, while the remaining were heated in a water bath at 52 ± 0.5 °C. Again, temperature stabilization was allowed before sintering was accepted to have started. Once the temperature had reached 49 ± 0.5 °C, the emulsion tubes were sintered for 5, 30, and 60 min, respectively. After sintering, the microcapsules were prepared for characterization. For each tube, 5 mL of emulsion was diluted with 35 mL of MilliQ water (18.2 MΩ•cm). This was then centrifuged at 10 000 rpm for 10 min at 20 °C. Most supernatant was removed by pipetting. Five milliliters of the supernatant and settled microcapsules were filtered with a 0.65 μm membrane in a Millipore filtration system. The collected microcapsules were then characterized.

2.2.5. Dye Encapsulation. To encapsulate a dye within the microcapsules, initially, fluorescein sodium salt (3.0 mg) was dissolved in 50 μL of MilliQ water (18.2 MΩ•cm) and mixed with the latex particle suspension (1.2 mL) to form the aqueous phase. Meanwhile, Span 80 (2.4 mL) was stirred in sunflower oil (120 mL) for 5 min with a Silverson mixer at 3000 rpm. Once both phases were ready, the aqueous phase was added into the oil over 30 s. Cyclic mixing was employed at 60 s homogenization, followed by 30 s rest, repeated five times. After emulsification, the emulsion was separated into three tubes and heated in a water bath at 50 °C. Once the temperature had stabilized at 49 ± 0.5 °C, the timer was started and the emulsions were sintered for 5, 30, and 60 min, respectively. The formed dye encapsulated microcapsules were kept in a darkened environment until used.

2.2.6. Dye Release Study. The dye-encapsulated microcapsules were left in the dark for one week to encourage gravity settling. At the end of the period, the "cleared" oil (30 mL) was removed by pipetting. The sedimented microcapsules were scraped off the tube wall and redispersed into the remaining oil (10 mL). The microcapsule suspension (5 mL) was then filtered through a Millipore glass vacuum filtration system with 0.65 μm membrane filter. Meanwhile, an amber 100 mL bottle was placed on a multiposition magnetic stirrer (IKA Werke GmbH & Co. KG, model RO5). Once filtration was completed, the filter was placed into the amber bottle and stirring was initiated. MilliQ water (30 mL, 18.2 MΩ•cm) was added to the bottle simultaneously while the timer was started. At specific intervals, 1 mL of dyed aqueous suspension was collected with a syringe and filtered through a 0.2 μm Whatman PTFE syringe filter into a 2 mL amber vial.

The dyed water was characterized by spectrophotometry. This was carried out in a UV−visible spectrophotometer equipped with a tungsten lamp (Thermo Scientific, model Heλios Gamma). The system was set at an excitation wavelength of 495 nm for 5 s measurements. MilliQ water (18.2 MΩ•cm) was used as a zero reference. Dyed water (0.3 mL) was injected into a 1 mm path length silica cuvette. The absorption value was recorded, and a graph of release yield against time was plotted. The dye release study was repeated with the remaining 5 mL microcapsule suspension to verify reproducibility.

2.2.7. Characterization Techniques for Colloidosomes. A Leica DME transmitted light microscope, coupled to an XLICap color digital camera and capture software (XLI Imaging Ltd., version 12.0), was used in the preliminary examination of the emulsions. This included water-in-oil microcapsules, dried water-in-water microcapsules, and oil-in-water microcapsules. The microcapsules were inspected under 10×, 20×, 40×, and 63× objectives. They were also examined under JEOL-6340F Field Emission Gun SEM at 5.0 kV. The microcapsules were air-dried on a stainless steel SEM stub overnight and then platinum-coated using an Emitech K575 sputter coater (argon environment, 1×10^{-3} mbar, 40 mA, 1 min).

From the optical images, the average size of the microcapsules was determined via image analysis with Aequitas IA software (Dynamic Data Links Ltd., version 1.4x). This program prepared binary images by manual editing to specify the desired objects for measurement. It then utilized pixel counting, comparing to a calibration scale of 1 mm stage micrometer, to give the particle size. One hundred objects were measured per batch to give the average diameter.

Sizing of the microcapsules was also performed via pulsed-field gradient nuclear magnetic resonance (PFG NMR). This was carried out with a 25 mm microimaging probe in a Bruker Avance DMX300 NMR spectrometer. The NMR spectrometer was coupled to a superconducting magnet of 7.05 T with proton frequency of 300.13 MHz. For the pulse sequence, the diffusion measurements were performed using alternating pulsed field gradient stimulated echo (APFG STE), with the gradient applied horizontally. This minimized any convection effect within the sample. A gradient was raised from 0 to 80 G/cm in 32 steps for a maximum time duration of 8 ms. All diffusion measurements were performed in

(20) Lee, W. P.; Routh, A. F. *J. Coatings Technol. Res.* **2006**, *3*, 301–307.

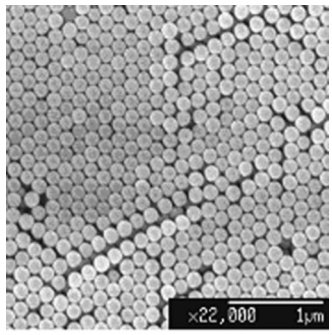

Figure 1. SEM image of latex particles.

observation times between 100 and 500 ms. From the NMR measurements, the size distribution of the microcapsules was obtained as described in Murday and Cotts,[21] Hrabe et al.,[22] and van Duynhoven et al.[23]

3. Results and Discussion

3.1. Poly(styrene-co-butyl acrylate) Particles. Styrene (65 wt %)/butyl acrylate (35 wt %) was the selected colloidal particle blend. The latex particles, made by emulsion polymerization, had an effective diameter of 180 ± 2 nm (by DLS) and a minimum film formation temperature of 42 °C (by MFFT bar). Figure 1 depicts a SEM image of the latex particles used in the colloidosome fabrication.

3.2. Water-in-Oil Colloidosomes. Colloidosomes are entities of liquid cores enveloped in shells of coagulated/fused colloidal particles.[10,24] They generally start as either water-in-oil or oil-in-water emulsion droplets. The fabrication principle lies in the minimization of interfacial energy that drives the colloidal particles to self-assemble at the water/oil interface. In addition, this stabilizes the emulsion droplets. Subsequently, sintering fuses the colloidal particles into a smooth, nonporous shell, giving the final microcapsule morphology.

Figure 2a illustrates an optical micrograph of water-in-oil colloidosomes. These microcapsules were subsequently washed and redispersed in an aqueous environment to give water-in-water microcapsules. They were then air-dried and imaged by optical microscopy, as depicted in Figure 2b as persistent dark rings. The phase transferred water-in-water microcapsules were also air-dried, platinum-coated, and examined under SEM. Figure 2c shows the successful formation of microcapsules. A close-up examination illustrates that the microcapsule had a shell of multiple coagulated 180 nm latex particles, arranged in a monolayer hexagonal grid fashion (Figure 2d).

From the optical images of the dried water-in-water microcapsules, an estimation of the average diameter of the microcapsules was determined using Aequitas IA. This gave an average diameter of 2.5 μm, from the measurement of 100 entities. The particle size distribution appeared broad due to the high shear emulsification technique employed, whereby the microcapsule size was governed by the shear force acting on the emulsion droplets during formation. Measurements were only accepted if the sphericity was above 0.9 and the actual area measured was above 0.5 μm^2. This assumed the microcapsules were perfectly spherical and excluded any flocculates of latex particles. This

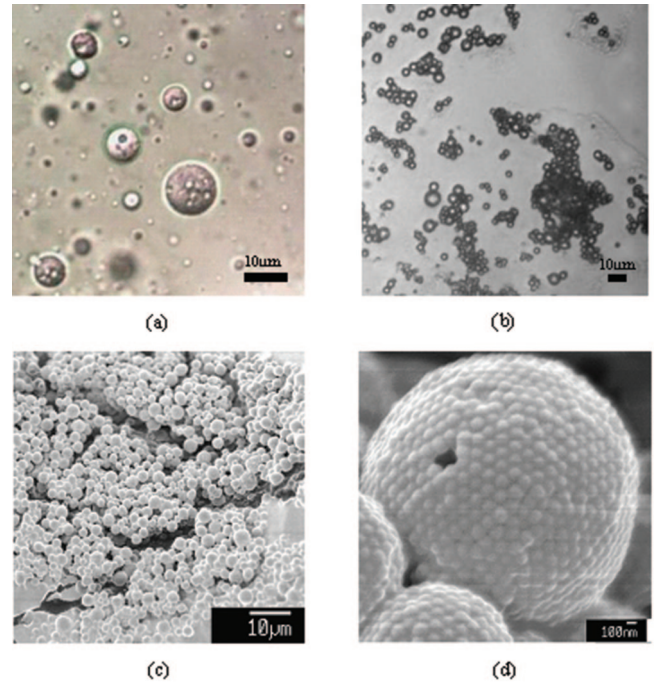

Figure 2. (a, b) Optical images of water-in-oil and dried water-in-water microcapsules, respectively. (c, d) SEM images of water-in-water microcapsules. All microcapsules were made with Span 80 at 3000 rpm and sintered for 5 min at 50 °C.

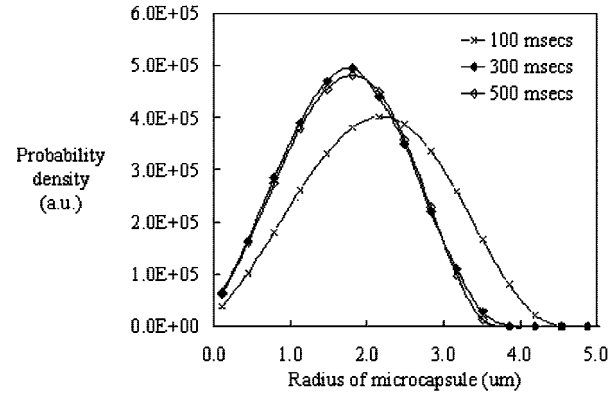

Figure 3. Size distributions of water-in-oil microcapsules by NMR measurements. The microcapsules were made with Span 80 at 3000 rpm and sintered for 60 min at 50 °C.

method aimed to avoid any optical errors and did not exclude any capsules.

The size distribution was further examined via NMR. The measurements were taken at three observation times, 100, 300, and 500 ms, as illustrated in Figure 3. A longer observation time gave more diffusion measurements, hence a more accurate sizing,[25] with the size of microcapsules being determined as 3.8 μm in diameter. The discrepancy between the diameters from Aequitas IA and NMR was probably due to the insufficient data points collected in Aequitas IA as a result of manual image manipulation. Also, it was subject to the location of microcapsule collection after gravity settling for Aequitas IA, whereas NMR looked at the whole emulsion with its simple, nonintrusive sample preparation.[23,26] Therefore, the size obtained by NMR was considered more accurate.

(21) Murday, J. S.; Cotts, R. M. *J. Chem. Phys.* **1968**, *48*, 4938–4945.
(22) Hrabe, J.; Kaur, G.; Guilfoyle, D. N. *J. Med. Phys.* **2007**, *32*, 34–42.
(23) van Duynhoven, J. P. M.; Goudappel, G. J. W.; van Dalen, G.; van Bruggen, P. C.; Blonk, J. C. G.; Eijkelenboom, A. P. A. M. *Magn. Reson. Chem.* **2002**, *40*, 51–59.
(24) Ashby, N. P.; Binks, B. P.; Paunov, V. N. *Phys. Chem. Chem. Phys.* **2004**, *6*, 4223–4225.
(25) Johns, M. L.; Hollingsworth, K. G. *Prog. Nucl. Magn. Reson. Spectrosc.* **2007**, *50*, 51–70.
(26) Hore, P. J. *Nuclear Magnetic Resonance. Oxford Chemistry Primers*; Compton, R. G. , Ed.; Oxford University Press Inc.: New York, 1995; p 90.

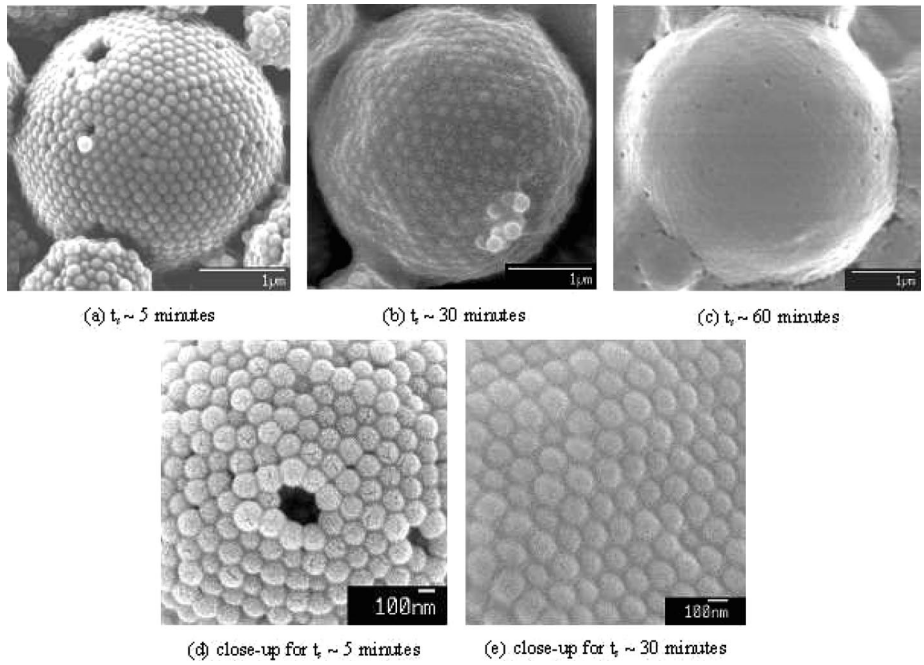

Figure 4. (a, b, c) Whole water-in-oil microcapsules at various sintering times. (d, e) Close-up into morphology of microcapsule shells. The microcapsules were made with Span 80 at 3000 rpm and sintered at various times at 50 °C. The close-up for $t_s \sim 60$ min appears as a white canvas under SEM and hence is not shown.

3.2.1. Effect of Sintering Time. Polymer sintering is defined as the formation of a homogeneous melt, as viscous particles deform under the action of surface tension.[27] The sintering process is governed by two factors: sintering time, t_s, and sintering temperature, T_s. Manipulation of these parameters allows control over the degree of fusing of colloidal particles, and hence the porosity and smoothness of the shell formed. Here, the effect of sintering time is investigated, while the subsequent section looks at the effect of sintering temperature.

Colloidosomes were sintered for 5, 30, and 60 min, respectively, at a constant temperature of 49 ± 0.5 °C. They were then subjected to similar oil-to-water phase transfer and air-dried for SEM. Figures 4a−c depict SEM images of microcapsules formed at various sintering times, with Figures 4d and 4e presenting a close-up of the morphology of the capsule shell. As observed from Figure 4, longer sintering times allowed formation of smoother shells. At a sintering time of 5 min, the individual latex particles were still clearly observed, giving shells with larger porosity. The term "porosity" is used to represent the ratio of the volume of interstitial spaces to the volume of latex particles or shell. Despite being considered as microcapsules with larger porosity at 5 min sintering, the interstitial spaces were indeed tiny as shown in Figure 4d. This was because the use of small soft polymeric particles (i.e., size ~ 180 nm, $T_g \sim 42$ °C) allowed closer packing of the particles, as they deformed into a hexagonal grid, and thus minimized the size of interstitial spaces. This is in contrast to the 1.1 μm polystyrene particles used to form colloidosomes in Hsu et al.[9]

As the sintering time progressed to 30 min, the latex particles began fusing into a film, with some remnants of latex particles still observable (Figure 4e). Once the sintering time reached 60 min, the microcapsules possessed smooth shells with latex particles fusing into a complete film, thus giving low porosity shells. The shell thickness was assumed constant throughout the sintering process, as migration of latex particles during fusing should be minimal due to the tiny interstitial spaces, as observed at 5 min sintering. This assumption is vital for the model fitting in the dye diffusion studies at later stages.

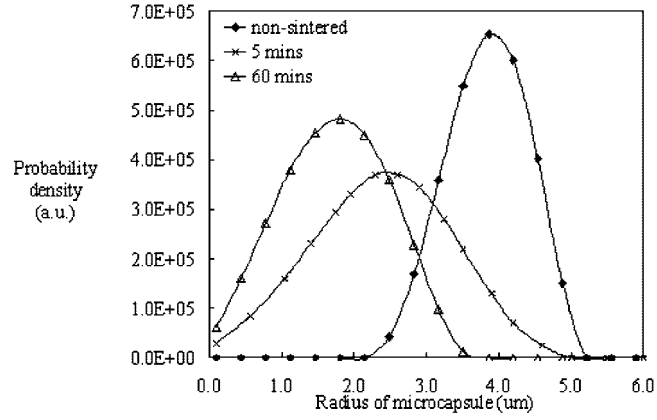

Figure 5. Size distributions of water-in-oil microcapsules at different sintering times. The microcapsules were made with Span 80 at 3000 rpm and sintered for various times at 50 °C.

PFG NMR was also employed to examine the effect of sintering time on microcapsule sizing. The measurements were taken at an observation time of 300 ms. Three sets of microcapsules were made: nonsintered microcapsules (i.e., no heating was applied), 5 min sintered (i.e., porous shell microcapsules), and 60 min sintered (i.e., smooth shell microcapsules). The size distributions of these microcapsules are presented in Figure 5. A distinct size difference was noted between nonsintered and sintered (t_s = 5, 60 min) microcapsules, whereby the average diameter of nonsintered ones at 8.0 μm was nearly twice the size of sintered microcapsules (4.8 μm for 5 min and 3.8 μm for 60 min microcapsules). This showed that over time the nonsintered colloidosomes experienced coalescence of their liquid cores, resulting in an increase of microcapsule size. Therefore, sintering is a key step in ensuring the locking of colloidal particles in place to form the capsule shell and maintain the microcapsule morphology.

(27) Bellehumeur, C. T.; Kontopoulou, M.; Vlachopoulos, J. *Rheol. Acta* **1998**, *37*, 270–278.

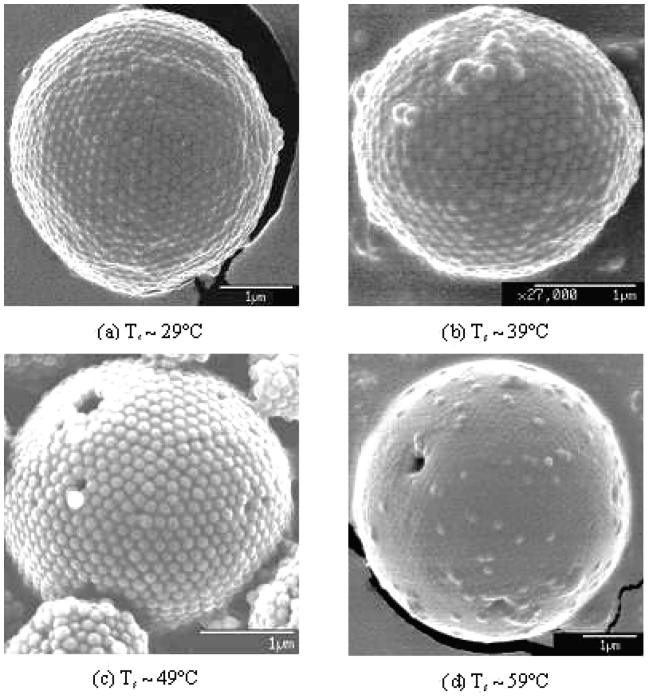

Figure 6. Case 1: water-in-oil microcapsules at various sintering temperatures. The microcapsules were made with Span 80 at 3000 rpm and sintered for 5 min at various temperatures.

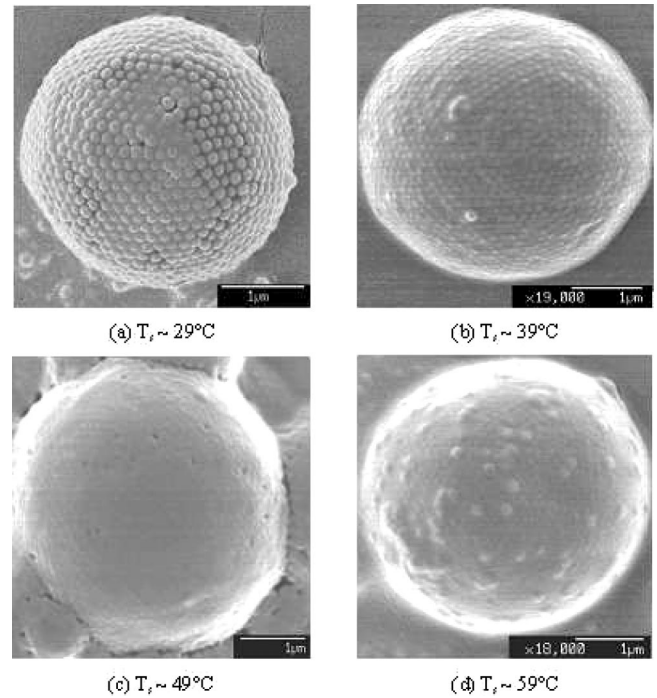

Figure 7. Case 2: water-in-oil microcapsules at various sintering temperatures. The microcapsules were made with Span 80 at 3000 rpm and sintered for 60 min at various temperatures.

3.2.2. Effect of Sintering Temperature. Sintering temperature has an effect on the colloidosome morphology because both surface tension and polymer viscosity are temperature-dependent properties. To study the effect of sintering temperature, colloidosomes were made at different temperatures: 29 ± 0.5 °C, 39 ± 0.5 °C, 49 ± 0.5 °C, and 59 ± 0.5 °C, while a constant sintering time was maintained. Two sintering times were investigated: 5 and 60 min. As determined earlier, the minimum film formation temperature, MFFT, of the latex particles was 42 °C. Hence, the variation in sintering temperatures encompassed both rigid polymer particles below the MFFT and film-forming particles above the MFFT. The colloidosomes were also subjected to similar oil-to-water phase transfer and air-dried for SEM.

Figures 6 and 7 depict two cases of colloidosomes formed at different sintering temperatures, while constant sintering times of 5 and 60 min, respectively, were maintained. It can be seen that as the sintering temperature increases, the degree of latex particle deformation increases accordingly. This is because as temperature increases, the polymer viscosity decreases dramatically.[28,29] This allows greater polymer particle fusion, and hence less porous shells. It should be noted that Figure 6c appears more porous than Figure 6b, contradicting the proposed rationale. This anomaly is attributed to the difficulty in obtaining a similar resolution for all SEM images, as the latex particles were prone to charging.

An interesting observation from this is the successful formation of colloidosomes despite sintering at temperatures below the MFFT. Even though the particles did not fuse together, they remain locked in a shell structure. This can be observed from Figures 6 and 7 (images a and b), which show the colloidosomes made at temperatures below MFFT. This is further verified in Figure 8, whereby the colloidosome depicted was formed without any heating and remained stable throughout the oil-to-water transfer and SEM processing. The individual latex particles in these circumstances were still distinctly evident, confirming the adsorption and locking of particles at the water/oil interface to form the shell. It should be noted that the PFG NMR results indicated that even though the shell appeared stable, the coalescence of cores still occurred over time, with a corresponding increase in microcapsule size.

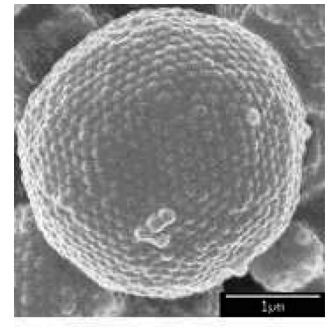

Figure 8. SEM image of a nonsintered water-in-oil colloidosome. The microcapsules were made with Span 80 at 3000 rpm, without any heating.

3.3. Oil-in-Water Colloidosomes. This section aims to demonstrate that using similar principles established for water-in-oil colloidosomes, it is indeed achievable to make the contrary system, i.e., oil-in-water colloidosomes. However, it should be noted that this contrary oil-in-water system still requires further improvement, as the system is not as clean as would be desired. Briefly, Tween 20 was added to the aqueous latex suspension. Emulsification with sunflower oil added into the aqueous phase resulted in an oil-in-water emulsion. Migration of the latex particles to the oil/water interface enabled stabilization of the emulsion droplets. Subsequent sintering locked the particles in place to form the oil-in-water microcapsules.

Figure 9a illustrates the oil-in-water microcapsules, imaged immediately after formation. The optical image shows a complex

(28) Routh, A. F.; Russel, W. B. *Langmuir* **1999**, *15*, 7762–7773.
(29) Funke, Z.; Schwinger, C.; Adhikari, R.; Kressler, J. *Macromol. Mater. Eng.* **2001**, *286*, 744–751.

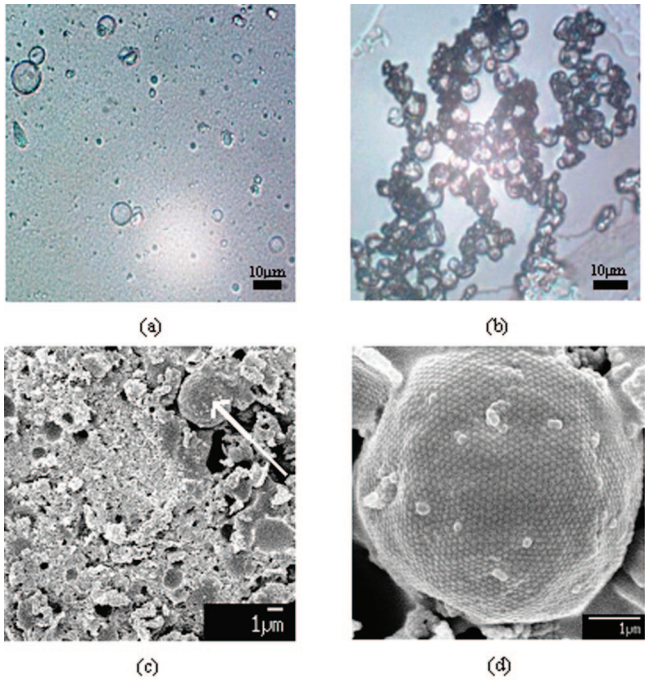

Figure 9. (a, b) Optical images of suspended and dried oil-in-water microcapsules, respectively. (c, d) SEM images of oil-in-water microcapsules. The microcapsules were made with Tween 20 at 6000 rpm and sintered for 5 min at 50 °C.

background made up of excess latex particles, with circular rings representing the formed microcapsules. This is further verified with Figure 9b, whereby the microcapsules remained evident despite centrifugation and drying. These microcapsules were then examined under SEM (Figures 9c and 9d). Figure 9c confirms the excess latex particles present, making it difficult to detect any formed microcapsules. As illustrated with an arrow, only a single microcapsule of 3.3 μm was detected within an image area of 20 × 20 μm. Meanwhile, Figure 9d portrays a close-up of an oil-in-water microcapsule, with the shell composed of multiple latex particles.

Through use of similar optical images to Figure 9b, Aequitas IA software was used to determine the average diameter of oil-in-water microcapsules. The process was more complicated compared to the water-in-oil system, due to the nonspherical entities and greater degree of flocculation. However, after manual binary editing of the images and measurements of 100 rings, it was determined that the average diameter of oil-in-water microcapsules was approximately 5.1 μm. Overall, this experiment proved that it was indeed possible to make oil−core and water−core microcapsules via the colloidosome route.

3.4. Dye Release Study. *3.4.1. Blank Tests.* Blank tests were carried out to investigate if any chemical reactions exist between sodium fluorescein dye and free-moving latex particles. The aim was to determine the maximum dye release from microcapsules. Three blank tests were done:

- blank 1—fluorescein dye (22 mg) in MilliQ water (20 mL, 18.2 MΩ•cm),
- blank 2—fluorescein dye (19 mg) and latex particles (50 μL, 5.6 wt % particle suspension in MilliQ water (20 mL, 18.2 MΩ•cm)), which was stirred for 1 min, and
- blank 3—same as blank 2, but heated at 50 °C for 1 h.

All mixtures were transferred into 10 cm of cellulose dialysis tubing (SpectraPor, MWCO: 12−14 kDa) and immersed in gently stirred MilliQ water (480 mL, 18.2 MΩ•cm). Samples of 0.3 mL each were collected at defined time intervals for spectrophotometry measurements. Figure 10 illustrates the dye release profiles for the blank tests. It can be clearly observed that the fluorescein dye had adsorbed onto the latex particles, resulting in only 65% dye release, compared to nearly 100% release for the pure dye case. This indicated that the maximum possible dye yield from subsequent dye-encapsulated microcapsules would be approximately 65−75% (considering the nonuse of dialysis tubing in later experiments). It should be noted that heating had no effect on the fluorescein−latex interaction.

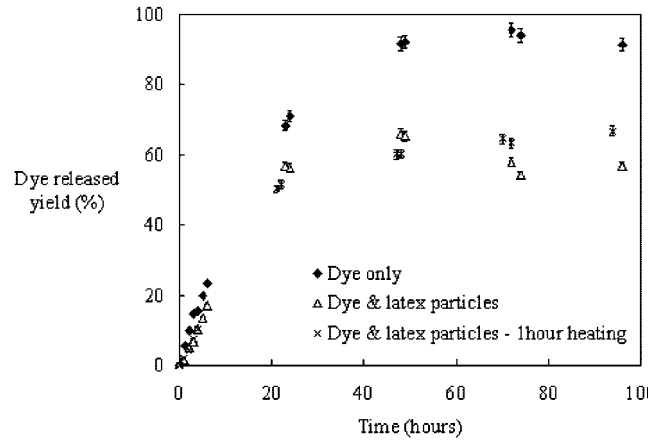

Figure 10. Results of blank dye test (data shown are mean ± SD for $n = 3$).

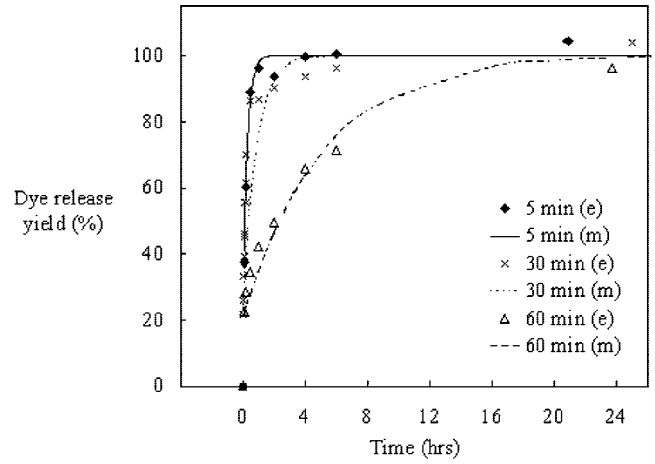

Figure 11. Dye release profiles with fitted model for encapsulated and maximum released fluorescein concentration of 2.51 and 0.0143 mM, respectively (data shown are mean values for $n = 2$). Symbols = spectrophotometry data, line = release model. The water-in-oil microcapsules were made with Span 80 at 3000 rpm and sintered for various times at 50 °C.

3.4.2. Encapsulated Dye Release Profiles. Previously, it was observed that for long sintering times, fusing of the shell latex particles was increased, and thus the shell became less porous. This provided a means to control the release rate of any encapsulated ingredient(s), with smoother shells requiring longer release times. A hydrophilic dye was encapsulated within water−core microcapsules, and the dye release profiles for microcapsules made at different sintering times were compared. Figure 11 illustrates the release profiles for encapsulated fluorescein dye in colloidosomes sintered at 50 °C for 5, 30, and 60 min, respectively. The profiles show the dye release yield, obtained by dividing the measured concentration with a known final value, against release time. Each release batch had a maximum released dye concentration of 0.0143 mM, as determined by the identical mass of dye used each time. This

corresponds to 75% of the total concentration due to the flourescein−latex interaction.

From Figure 11, 60 min sintered microcapsules exhibited the slowest release profile, with 5 and 30 min microcapsules showing nearly identical release profiles. The slowest release by 60 min microcapsules was expected, as at this point the shell was completely sealed with the least permeable structure. However, the marginally slower release profile from 30 min microcapsules, compared to 5 min release, was more surprising. This could be explained by the existence of remnant shell latex particles for the 30 min microcapsules (Figure 4b), indicating a porous shell structure might still remain. The steep 5 min release profile, on the other hand, was due to the relative higher porosity in the 5 min microcapsules (Figure 4a), with some having hole(s) within the shells. The presence of these holes would encourage quicker dye release initially. However, given the interest is in the attainment of an equilibrium for the dye release over 24 h, this effect would be minimal in the overall process as well as in the estimation of the diffusion coefficient in the subsequent section.

3.4.3. Dye Release Model Fitting. To fit the release profiles, it is necessary to solve the unsteady diffusion equation in spherical coordinates for a sphere of radius R and shell thickness b. A simple approach is to assume that the concentration of fluorescein dye in the core of the microcapsules changes slowly with respect to the diffusion through shell, which ascertains to a steady state profile. The dye concentration profile across the shell, c, at radius r is given by

$$c = \frac{C_{in}R(R+b)}{br} - \frac{C_{in}R}{b} \quad (1)$$

where C_{in} is the slowly varying concentration in the core. The exudation of material, j, is therefore a constant radially and given by

$$j = 4\pi D\frac{C_{in}R(R+b)}{b} \quad (2)$$

with D the diffusion coefficient of dye in the microcapsule shell. A conservation equation for fluorescein dye then provides the core concentration as a function of time t and is given by

$$C_{in} = C_{in(0)}\exp\left(-\frac{3D(R+b)}{R^2b}t\right) \quad (3)$$

Hence, the total amount of dye released from each microcapsule as a function of time, M, is determined by integrating the exudation expression in eq 2 with eq 3 for the core concentration. The final answer is

$$M = \frac{4\pi R^3}{3}C_{in(0)}\left(1-\exp\left(-\frac{3D(R+b)}{R^2b}t\right)\right) \quad (4)$$

The experimental data indicated almost 20% of the fluorescein dye was released very quickly, at least before the first measurement could be made. We ascribe this to the free dye attached to the outside of the microcapsules and any imperfection in the capsule shells, thus allowing quick release.[30,31] So, the percentage of fluorescein released, $M_{\%}$, can be fitted as

$$M_{\%} = 80\left(1-\exp\left(-\frac{3D(R+b)}{R^2b}t\right)\right)+20 \quad (5)$$

Figure 11 depicts the fitting of eq 5 to the spectrophotometry data in a plot of $M_{\%}$ against time. There is good correlation between theory and experimental data. From the fit, it was

Table 1. Dye−Shell Diffusion Coefficients for Water-in-Oil Microcapsules Made with Span® 80 at 3000 rpm and Sintered at 50 °C at Various Durations

sintering time, t_s (min)	fitted dye−shell diffusion coefficient, D ($\times 10^{-17}$)(m^2/s)
5	11.1
30	3.5
60	0.6

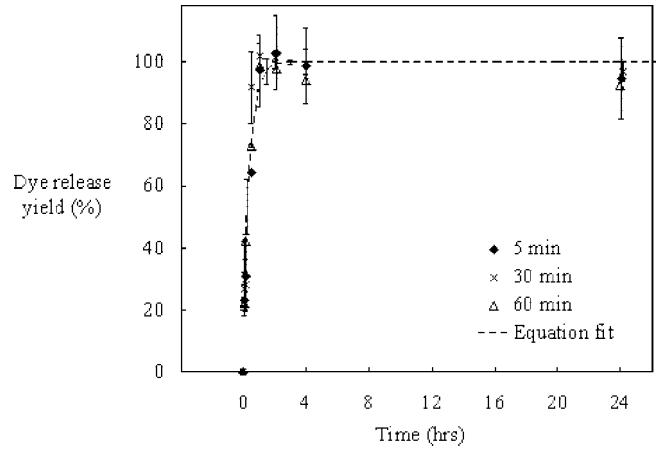

Figure 12. Equation fitted profile for encapsulated and maximum released fluorescein concentration of 7.65 and 0.0434 mM, respectively (data shown are mean ± SD for $n = 2$). Symbols = spectrophotometry data, line = release model. The water-in-oil microcapsules were made with Span 80 at 3000 rpm and sintered for various times at 50 °C.

observed that an increase in sintering time for colloidosomes produced a slower fluorescein−shell diffusion coefficient (Table 1). This was consistent with the SEM images (Figure 4), whereby longer sintering times allowed greater fusing of the latex particles in the shell. This led to reduced permeability of the shell and, hence, slower release of the dye from its encapsulated state. Unfortunately, there are limited literature data available for comparison. Song et al. obtained a diffusion of fluorescein in nylon-66 of the order 10^{-15} m^2/s,[32] which is comparable to the experimental fluorescein poly(styrene-*co*-butyl acrylate) coefficient of 10^{-17} m^2/s.

An alternative approach to model these experimental results is to employ the diffusion model by Berg,[33] which proposes that diffusion only takes place through the circular apertures in a nonpermeable barrier. To apply this model, it is necessary to estimate the number of apertures per unit area as well as the aperture radius. Both these "free" parameters have been accounted for in our proposed diffusion coefficient, D, allowing a single parameter model. It is indeed possible to infer an aperture size from Berg's model; however, this again is only valid as a rough estimation, given the number of variables involved.

3.4.4. Effect of Encapsulated Dye Concentration. The dye release study was repeated with a higher dose of encapsulated fluorescein dye of 7.65 mM. This gave a maximum released dye concentration of 0.0434 mM, which was three times higher than the previous experiment. This study was aimed at investigating the effect of dye concentration on colloidosome formation, as the adsorption of fluorescein onto latex particles might affect the formation stability. Figure 12 illustrates the dye release profiles for microcapsules with the higher fluorescein concentration. The

(30) Khopade, A. J.; Caruso, F. *Biomacromolecules* **2002**, *3*, 1154–1162.
(31) Choucair, A.; Lim, P. S.; Eisenberg, A. *Langmuir* **2005**.
(32) Song, Y.; Srinivasarao, M.; Tonelli, A.; Balik, C. M.; McGregor, R. *Macromolecules* **2000**, *33*, 4478–4485.
(33) Berg, H. C. *Random Walks in Biology*; Princeton University Press: Princeton, NJ, 1983; p 137.

microcapsules were fabricated at 50 °C at sintering times of 5, 30, and 60 min, respectively. They had an 85% maximum released dye concentration, relative to the theoretical prediction. The additional 10% release could be attributed to the presence of a higher initial fluorescein dye concentration, allowing for saturation within the polymeric shell and, hence, a higher release yield.

From Figure 12, the release profiles were almost identical, at least within experimental error. This was verified with the fitting of eq 5, whereby a single fluorescein−shell diffusion coefficient, D_s, of 6.7×10^{-17} m^2/s was able to represent all three release profiles. The value of 6.7×10^{-17} m^2/s was comparable with the values obtained for 5 and 30 min sintering at the lower fluorescein dye concentration. This implied that the interstices or defects in the capsule shell were controlling the mass transfer and sintering was not capable of removing these holes. This result indicates that the encapsulated dye concentration has a direct effect on the latex particles and thus affected the microcapsule shell formation. This is explainable by salt-induced colloidal aggregation,[17,34] whereby addition of an inert electrolyte screens the surface charge of particles in suspension. This reduces the electrostatic barrier that promotes colloidal stability. This simultaneously encourages the aggregation of latex particles, which reduces the number of particles available for self-assembly at the water/oil interface. Therefore, the higher dye concentration induces more particle aggregation and, therefore, more defects in the microcapsule shells.

4. Conclusions

Low temperature colloidosomes were successfully fabricated by self-assembling latex particles (MFFT = 42 °C) at the interface of both water-in-oil and oil-in-water emulsion droplets. Subsequent sintering at 50 °C locked the particles in place and eventually formed smooth shells. The permeability of microcapsule shells was investigated by controlling the sintering time and temperature. For a given temperature, longer sintering times enabled formation of less porous shells, until smooth shells were eventually developed. This observation was further investigated through the release profiles of an encapsulated dye from the aqueous microcapsule cores. It was demonstrated that longer sintering times resulted in slower release of the encapsulated ingredient, supporting the finding of less permeable shells at longer sintering. The diffusion equation for spherical structures was fitted to describe the dye release event, and the diffusion coefficient of fluorescein dye through the polymeric shell was estimated as 10^{-17} m^2/s. For a given sintering time, increasing the temperature gradually resulted in smoother shells. An interesting observation was the formation of intact colloidosomes despite heating at temperatures below the MFFT. This was substantiated by the successful formation of colloidosomes even when no heating was applied. However, coalescence of colloidosomes occurred when heating was not applied, as picked up by NMR, showing nonsintered microcapsules to be twice the size of sintered ones.

Acknowledgment. The authors would like to thank Yasar Khan and Dr. Mike Johns for their help with NMR measurements. Also, the authors would like to thank EPSRC for grant GR/T28942/01. H.N.Y. is a recipient of an Overseas Research Studentship award.

LA802711Y

(34) Kjoniksen, A. L.; Joabsson, F.; Thuresson, K.; Nystrom, B. *J. Phys. Chem. B* **1999**, *103*, 9818–9825.